

Notched Strip Tensile Tests to Determine the Yield Characteristics of Stainless Steel

Jurgen Becque, Ajibola Oyawoye, Maurizio Guadagnini, Shan-Shan Huang

Department of Civil and Structural Engineering, The University of Sheffield, Sheffield, UK

Abstract

The paper investigates the use of notched strip tensile tests, originally proposed by R. Hill, to determine the yield characteristics of stainless steel. The original concept is thereby improved in two important ways. First of all, digital image correlation techniques are used to allow an accurate measurement of strain rates in a very localized area. Second, new theoretical developments are presented, which eliminate the need for measuring the applied load and which allow the yield surface of an anisotropic material to be determined starting from a parameterized equation. An experimental program is described where the method has been successfully applied to a ferritic grade as well as an austenitic grade stainless steel. As a disadvantage, a relatively large scatter in test results appears to be intrinsic to the method of notched strip tests.

Keywords

notched strip, yield surface, stainless steel, combined tension and shear, anisotropy

1 Background

Experimentally determining the yield characteristics of a metal in combined tension and shear is a task which is not easily accomplished. Two methods to achieve this are commonly used and well documented in literature. They both involve a circular tube which is either subjected to internal pressure in combination with torsion (Taylor and Quinney 1932, Schmidt 1932), or to combined axial loading and torsion (Lode 1926, Davis 1943, Fraenkel 1948). Both methods require a complicated test apparatus which may not be part of the inventory of a typical structural research facility. Moreover, these methods are impractical for flat plate materials since they imply the fabrication of a tube by cold-forming and welding, both of which may alter the material properties. The search for an alternative test method is therefore a more than worthwhile undertaking.

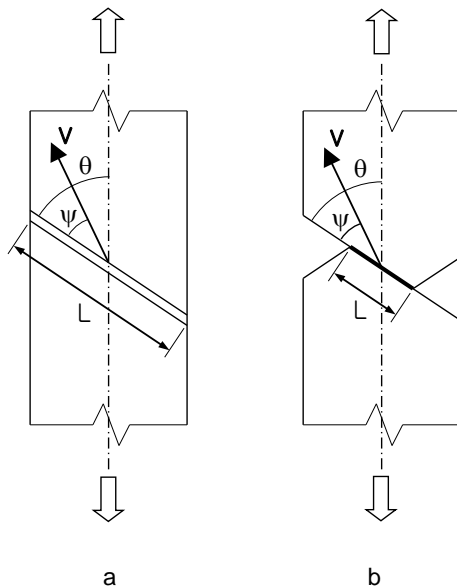


Figure 1 Grooved and notched strip specimens

Bijlaard (1940) was first to propose the ingenious idea of using strips with a diagonal weakened cross-section pulled in simple tension to impose a state of combined shear and tension onto the material (Figure 1a). The weakened cross-section was thereby achieved by locally reducing the thickness of the material. This method, while a possible option, requires a high degree of accuracy and control during the cutting of the grooves in order to obtain uniform dimensions. Hill (1953) therefore proposed the alternative of cutting asymmetric notches in the strip, thereby forcing the material to yield along a straight narrow zone connecting the roots of the notches (Figure 1b). The notches have to be sufficiently deep and sharp to localize the yielding along this neck, of which the width is of the order of the thickness of the plate material (Hill 1953). The great advantage of this concept lies in its simplicity. The yield characteristics of the material

in combined shear and tension can be determined from a simple uniaxial tensile test. Moreover, the notched strips are easily manufactured.

The angle θ , as indicated in Figure 1, is measured between the neck and the longitudinal axis of the tensile specimen and may be varied between 55° and 90° . The lower-bound value of 55° corresponds to a state of pure tension in the neck, as it is the angle at which a neck would develop in a straight tensile specimen without notches (Hill 1952). When a neck develops and both sides of the specimen start sliding relative to each other along the narrow yield zone formed by the neck, the angle of the relative velocity ψ is measured (Figure 1). More specifically, ψ is defined as being the angle included between the neck and the relative velocity vector \mathbf{v} .

The mathematical theory behind the necking of strips pulled in tension was developed by both Bijlaard (1940) and Hill (1953). It is assumed that the material is perfectly rigid-plastic and that the two halves of the specimen slide relative to each other as rigid bodies once the neck develops. The theory also assumes that the material is isotropic, so that the principal directions of stress and plastic strain rate coincide. Under those assumptions the ratio of the principal stresses in the neck, which depends on θ and ψ , is given by:

$$\frac{\sigma_1}{\sin(\theta - \psi) + \cos \theta} = \frac{\sigma_2}{\sin(\theta - \psi) - \cos \theta} = \frac{P}{tL \cos \psi} \quad (1)$$

In Eq. (1), t is the material thickness, L is the length of the neck (equal to the straight distance between the roots of the notches) and P is the value of the applied load which causes the neck to form.

On the other hand, the ratios between the principal strain increments in the neck are given by:

$$\frac{\dot{\epsilon}_1}{1 + \sin \psi} = \frac{\dot{\epsilon}_2}{\sin \psi - 1} = \frac{\dot{\epsilon}_3}{-2 \sin \psi} \quad (2)$$

Eqs. (1) and (2) allow for Lode's parameters μ and ν to be calculated:

$$\mu = -\frac{\sigma_1 + \sigma_2}{\sigma_1 - \sigma_2} = -\frac{3 \cos \theta - \sin(\theta - \psi)}{\cos \theta + \sin(\theta - \psi)} \quad (3)$$

$$\nu = \frac{2\dot{\epsilon}_2 - \dot{\epsilon}_1 - \dot{\epsilon}_3}{\dot{\epsilon}_1 - \dot{\epsilon}_3} = -\frac{3(1 - \sin \psi)}{1 + 3 \sin \psi} \quad (4)$$

In stress space the parameter μ determines the angle β in the deviatoric plane between the stress vector and the direction of pure shear $\sigma_2 = -\sigma_1$ through the equation (Hill 1950) (Figure 2):

$$\mu = -\sqrt{3} \tan \beta \quad (5)$$

Similarly, ν determines the angle γ in the same stress space between the plastic strain rate vector and the direction $\mu = 0$ (Hill 1950):

$$\nu = -\sqrt{3} \tan \gamma \quad (6)$$

If the material is isotropic and obeys the von Mises criterion, then the plastic strain rate vector and the deviatoric stress vector are collinear due to the associativity of the flow rule and $\mu = \nu$. If θ and ψ pairs are obtained from notched strip tests, then Eqs. (3) and (4) can be used to perform a check on whether the material does indeed obey the von Mises criterion.

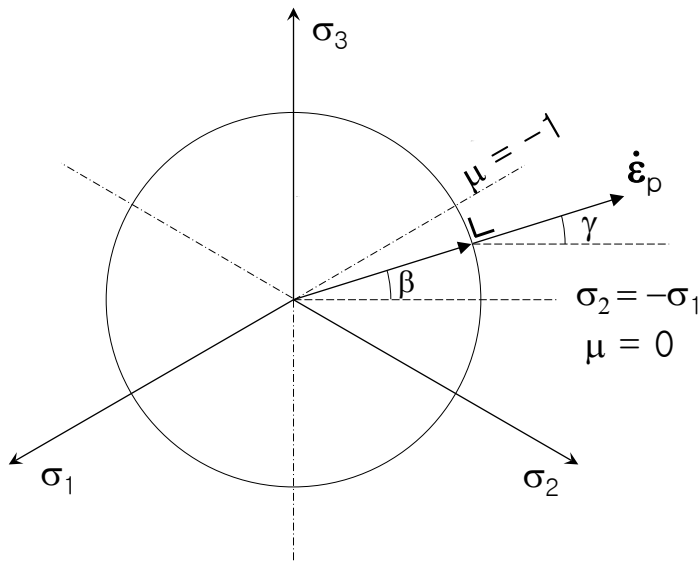


Figure 2 Yield surface in the deviatoric plane

Using Eq. (1), the length of the stress vector in the deviatoric plane is:

$$\sqrt{\frac{2}{3}(\sigma_1^2 - \sigma_1\sigma_2 + \sigma_2^2)^{\frac{1}{2}}} = \sqrt{\frac{2}{3}} \frac{P}{tL \cos \psi} [\sin^2(\theta - \psi) + 3 \cos^2 \theta]^{\frac{1}{2}} \quad (7)$$

If the load P causing necking in the strip is also measured during tests for different θ and ψ pairs, then Eq. (7) allows, in principle, for the shape of the yield surface in the deviatoric plane to be plotted. It thereby suffices to vary the angle θ of the neck between 55° and 90° , thereby varying μ between -1 (corresponding to a state of pure tension) and 0 (corresponding to a state of pure shear) to obtain a complete picture of the yield surface, because of its six-fold symmetry in the deviatoric plane about the projected σ_1 , σ_2 and σ_3 axes, as well as about the lines perpendicular thereto (Hill 1953) (Figure 2). However, Eqs. (1), and, as a result, Eq. (7), are implicitly based on the assumption that the material yields isotropically, a condition which has to be satisfied in order to arrive at a valid result.

An experimental implementation of Hill's ideas came as early as 1954 and was carried out by Hundy and Green (1954) at the British Iron and Steel Research Association in Sheffield. The researchers tested notched strips of copper, zinc and an austenitic grade 18/8 stainless steel (no further details on the metallurgy or chemical composition were provided). Special care was taken to produce specimens which were as isotropic as possible. The strips were reduced in thickness by rolling and annealed after each 15-20% reduction. Before annealing, the strips were also roller leveled with the aim of moderating any preferential orientation introduced by the rolling. Regular tensile coupons were cut under different angles with the rolling direction and the materials were found to be close to isotropic, with the possible exception of copper, which displayed slightly more anisotropy. Eleven notched strip specimens were tested for each metal with angles θ ranging from 55° to 90° . It was concluded from the tests that $\mu = \nu$ in close approximation for all three metals and that they therefore obeyed the von Mises criterion.

Lianis and Ford (1957) carried out 17 notched strip tests on commercially pure aluminium. The strips were rolled down at the temperature of liquid air to give it the properties of a near perfectly plastic metal. It was concluded from the tests that, within experimental scatter, the Lode's parameters were equal: $\mu = \nu$. Eq. (7) was used to plot the yield surface and all test points were found to fall within 3% of the von Mises surface. These conclusions were reinforced by regular tensile coupon tests in different directions relative to the rolling direction indicating no anisotropy.

Ellington (1958) applied the concept of grooved specimens to copper and alpha brass. In the case of alpha brass μ was found to be equal to ν . However, for copper this was not the case, a fact which was attributed to anisotropy in the material.

Baraya and Parker (1963) conducted tests on notched specimens of half-hard aluminium, varying the angle θ between 55° and 80° . They found that, within scatter, $\mu = \nu$. Tensile coupon tests at varying angles with the rolling direction showed a variation of up to 2.5% from the average tensile strength, indicating negligible anisotropy.

After this initial flurry of experimental activity between 1954 and 1963, it appears that research on the topic stalled. No evidence was found in literature of researchers having used the method since. The fact that the concept was largely

abandoned can be attributed to a number of fundamental problems with the method of practical as well as theoretical nature:

First of all, the method hinges on the accurate measurement of the angle ψ which determines the orientation of the relative velocity vector. This poses a considerable experimental challenge. In early experiments, Bijlaard (1940) attached a pen to the material on one side of the neck, which left a trace on the material on the other side of the neck. Hundy and Green (1954), however, developed a more accurate way to measure ψ by scribing a fan of lines over the neck at, for instance, 1° intervals (Figure 3). When the neck develops, two halves of a line on opposite sides of the neck undergo a relative lateral displacement unless the line coincides with the direction of relative motion. By measuring the relative lateral displacement of each line with a traveling microscope, an accurate value of ψ can be interpolated. Hundy and Green estimated the accuracy of their method at 0.5° . Baraya and Parker (1963) noted that errors result from the scribed lines not being perfectly straight and uniform in thickness and fine-tuned the technique further. They first scribed the fan of lines on a coated glass plate using a diamond scribe on a jig borer. Using a fairly complicated photographic printing process and a special dye, the image was then transferred to the specimens. It was demonstrated that the technique did lead to a more accurate determination of ψ . However, the added complexity associated with determining ψ with sufficient accuracy significantly takes away from the original goal of having an easy-to-carry-out, inexpensive test within reach of a basic testing facility.

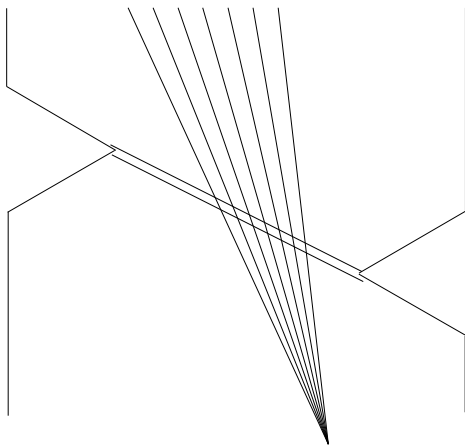


Figure 3 Fan of lines to aid in determining ψ

Second, in materials with significant strain hardening a localized neck may not develop, but instead a diffuse neck forms. This phenomenon pre-empted Baraya and Parker (1963) from testing notched specimens of certain aluminium alloys (2SO and 3SO). Hill (1952) mathematically worked out the conditions under which a localized neck develops in a strain-hardening material. It is generally accepted that an initial diffuse neck is permissible, provided that it becomes localized as plastic deformation progresses and as the amount of strain hardening typically decreases at higher stress levels. This is supported by the observation that the angle ψ typically remains fairly constant as plastic deformations in the neck progress (Hundy and Green 1954).

Third, brittle fracture might occur in the specimen, originating from the stress concentrations at the roots of the notches. This was experimentally observed by Baraya and Parker (1963) in several aluminium alloys (in particular: 24ST and B51SWP). Fracture thereby occurred at right angles with the specimen axis. Hundy and Green (1954) observed a related problem for the case of mild steel, where yielding propagated from the roots of the notches at right angles with the longitudinal axis.

A fourth problem relates to the application of Eq. (7). Lianis and Ford (1957) were able to employ Eq. (7) in order to arrive at a plot of the yield surface. However, they managed to do so for an aluminium alloy with near perfect plasticity. The presence of strain hardening typically causes the load-extension curve obtained from the test to become rounded, as illustrated in Figure 4 for the austenitic AISI 304L stainless steel employed in our test program. It is practically very difficult in strain hardening materials to obtain a reliable measurement of P , the load causing localized yielding in the neck. Hundy and Green (1954) stated they were unable to determine the yield surfaces of all three metals tested (copper, zinc and stainless steel) because of the roundness of the load-extension diagram. Baraya and Parker (1963) plotted the yield surface of half-hard aluminium, but noticed it deviated considerably from the von Mises surface: a clear

contradiction with their earlier finding that $\mu=v$ for this material ! It caused them to conclude that ascertaining a yield surface through this method is, in their words, ‘an elusive affair’.

Unfortunately, this limits the practicality of notched strip tests for strain hardening materials to a test on whether the material is approximately isotropic or not, through determining whether $\mu=v$.

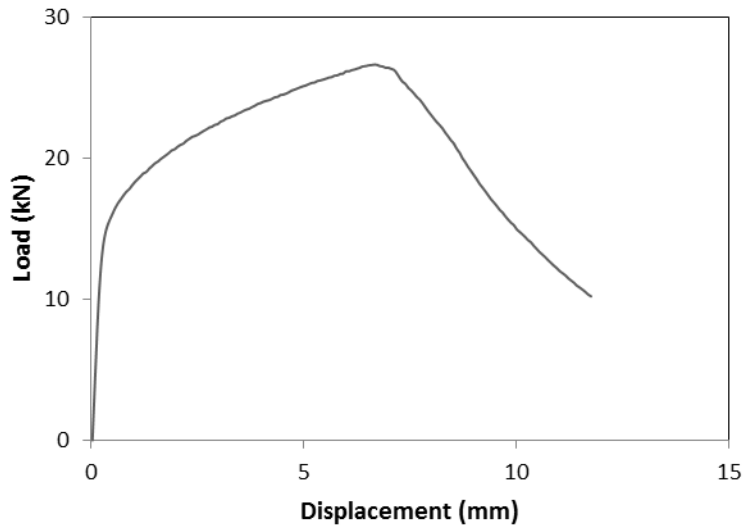


Figure 4 Load-displacement curve

Finally, the mathematical theory behind the concept only applies to isotropic materials. Due to the lack of an equivalent anisotropic theory no information can currently be deduced from a notched strip test on an anisotropic material (except, of course, that it is anisotropic).

This investigation was aimed at reviving the concept of notched strip tests by addressing the aforementioned issues. The particular focus was thereby on stainless steel alloys. Ideally the improved test method should satisfy three criteria originally set out by Hill (1953): 1. A simple test apparatus, 2. Easily manufactured test specimens, and 3. An easy test procedure, including easy and reliable data measurements.

The measurement problem of accurately determining ψ was confronted using the relatively new technique of DIC (Digital Image Correlation). In DIC, photographs are taken of the test specimen at regular intervals and an algorithm correlating subsequent images is then used to calculate relative displacements and strains.

Problem two is obviously material related, although deeper notches may help in localizing the yielding. Austenitic grades of stainless steel typically display a significant amount of strain hardening, while ferritic grades exhibit this property to a lesser amount. A short feasibility study was carried out at the start of the investigation using the finite element software ABAQUS v6.10 (2010). A notched strip with a geometry previously used successfully by Hundy and Green (1954) and Lianis and Ford (1957) was modelled using 3D 20-node brick elements. The depth of the notches (25 mm) was 1/3 of the width of the strip (75 mm), while the notches had the shape of equilateral triangles. Four notches were used symmetrically, allowing two necks to develop simultaneously and clamped ends to be used. The angle θ was taken as 60° . The mesh was sufficiently refined around the location of the neck (Figure 5). The stress-strain curve of the material was modelled using a Ramberg-Osgood equation:

$$\varepsilon = \frac{\sigma}{E} + 0.002 \left(\frac{\sigma}{\sigma_{0.2}} \right)^n \quad (8)$$

where the elastic modulus $E = 200$ GPa, the 0.2% proof stress $\sigma_{0.2}$ was assumed to be 280 MPa and the roundness parameter n was taken as 7, these values being typical of an austenitic stainless steel (Becque 2009). The results of the analysis are pictured in Figure 5, which shows a. the von Mises stresses and b. the magnitude of the displacement vector, after sufficient longitudinal extension has taken place. It is clear that localized necking indeed develops, with parts of the specimen on either side of a neck moving relative to each other as rigid bodies in very close approximation. Sufficient confidence was gained from this to proceed with the investigation. A ferritic grade stainless steel, as well as an austenitic grade were considered in the investigation in order to study whether their different strain hardening properties have a different effect on the notched strip tests. The ferritic grade considered was 1.4301 according to EN

10088-1 (2005), equivalent to type 304L according to the AISI classification (1974). The austenitic grade was 1.4016 according to EN 10088-1 (2005), equivalent to type 430 according to the AISI classification (1974).

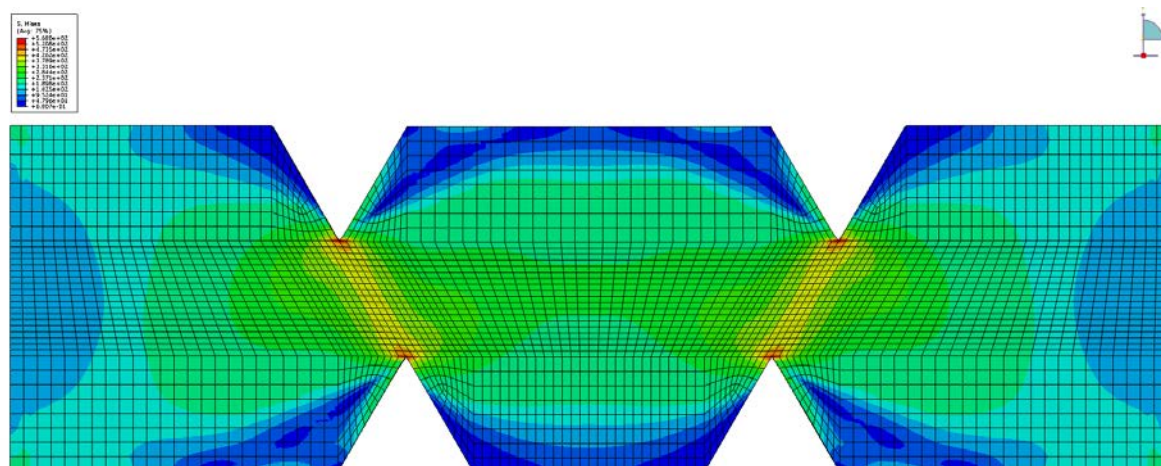


Figure 5a Von Mises stresses after formation of the neck

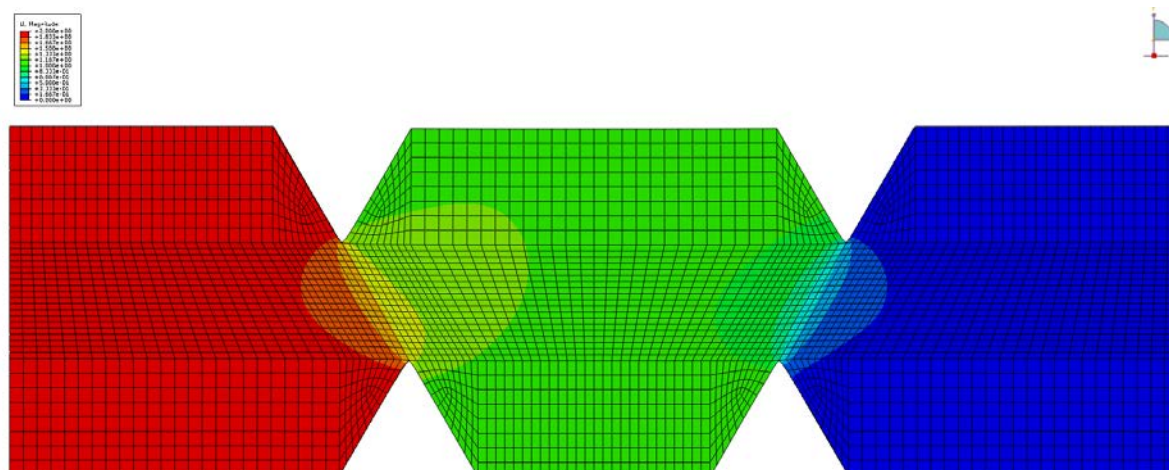


Figure 5b Magnitude of the total displacements after formation of the neck

With respect to the issue of brittle failure, Figure 5a clearly shows very significant stress concentrations at the roots of the notches, with von Mises stresses in this case about 40% higher at the notch tips than they are in the middle of the neck. On the other hand, the remarkable ductility typically encountered in austenitic stainless steels, and to a lesser extent in the ferritic grades, reduces the probability of brittle fracture. The notched strip specimens used in our investigation were laser-cut, to avoid overcutting or the introduction of stress concentrations and small defects at the roots of the notches due to machining.

Problems four and five reveal a need for further theoretical developments. In a first step, it is noted that it is not strictly necessary to measure the load P at which necking develops, in order to obtain the yield surface of the material. The first equality in Eq. (1) defines the ratio of the stresses σ_1 and σ_2 , and consequently the angle β (Figure 2), while the ratios of the principal (plastic) strain rates (and consequently the flow rule) is determined by Eq. (2). As a result of the associativity of the flow rule, the normal to the yield surface, as well as the line tangential to the yield surface, are then known. In principle, the yield surface can be reconstructed from tangential segments, provided a sufficient number of test points are available and provided a starting point on the yield surface is known e.g. from a uniaxial tensile test. A more practical approach, however, consists of proposing an equation for the yield surface containing a number of parameters and then to determine those parameters by aligning the normal vectors to the surface with the plastic flow vectors determined from test data through Eq. (2). The theory proposed in the next section is based on this principle and is sufficiently general to include the case of anisotropic materials.

2 Theory

We maintain the assumption of a rigid-plastic material and neglect the elastic strains with respect to the plastic strains. We also adopt Hill's (1950) anisotropic yield criterion, which, in the case of plane stress, reduces to an expression with four parameters F, G, H and N:

$$F\sigma_y^2 + G\sigma_x^2 + H(\sigma_x - \sigma_y)^2 + 2N\tau_{xy}^2 = \sigma_0^2 \quad (9)$$

On an important note, Eq. (9) is only valid as long as the x- and y-axes coincide with the principal axes of anisotropy in the material. In what follows, we assume the y-axis to coincide with the rolling direction of the plate and the x-axis to correspond to the direction transverse to the rolling direction. In Eq. (9), the reference stress σ_0 is taken to be the yield stress in the rolling direction. Eq. (9) reduces to the well-known von Mises criterion for $F=G=H=0.5$ and $N=1.5$.

It is also noted that other parameterized expressions may be proposed for the yield surface and that it would be straightforward to modify the theory here proposed accordingly.

The assumption of plane stress is satisfied as long as the variation in thickness along the deformed specimen is sufficiently small. This can reasonably be expected at the onset of necking.

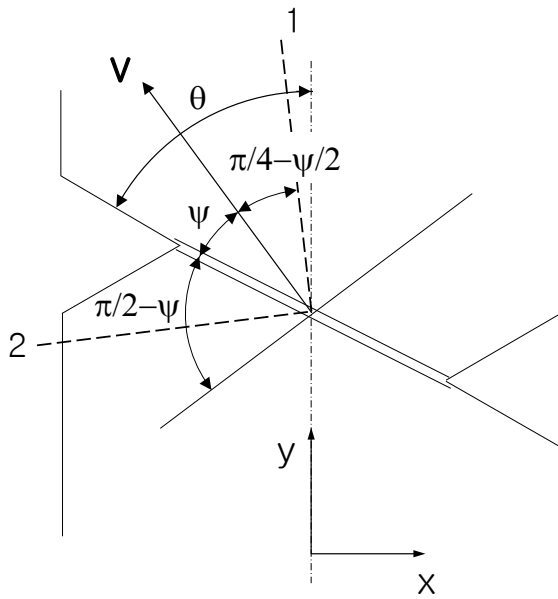


Figure 6 Principal directions of strain rate in the neck

We now consider the specimen at the onset of necking (Figure 6). Two directions can be identified along which the rate of normal straining is zero: 1. the direction perpendicular to the relative velocity vector, and 2. along the neck, since the material adjacent to the neck is assumed to remain rigid. Based on these observations, Mohr's circle of the plastic strain rates can be constructed (Figure 7a) and the principal directions of plastic strain rate identified. Despite the absence of a plane strain rate situation, Mohr's circle may be used to rotate the reference frame about the normal to the specimen, because this is a principal direction of plastic strain rate. The radius of Mohr's circle is given by $v/2b$, where v is the magnitude of the relative velocity and b is the width of the neck. This follows from the normal strain rate in the direction of \mathbf{v} being equal to:

$$\dot{\epsilon}_v = \frac{v}{b/\sin \psi} \quad (10)$$

Figure 7a indicates the directions of the neck (N), the vector \mathbf{v} (V) and the longitudinal axis of the specimen (Y), which is assumed to coincide with the rolling direction y , in Mohr's diagram. The plastic strain rates in the x-y reference system are thus:

$$\dot{\epsilon}_x = \frac{v}{2b} [\sin \psi - \sin(2\theta - \psi)] \quad (11)$$

$$\dot{\varepsilon}_y = \frac{v}{2b} [\sin \psi + \sin(2\theta - \psi)] \quad (12)$$

$$\dot{\varepsilon}_{xy} = \frac{v}{2b} \cos(2\theta - \psi) \quad (13)$$

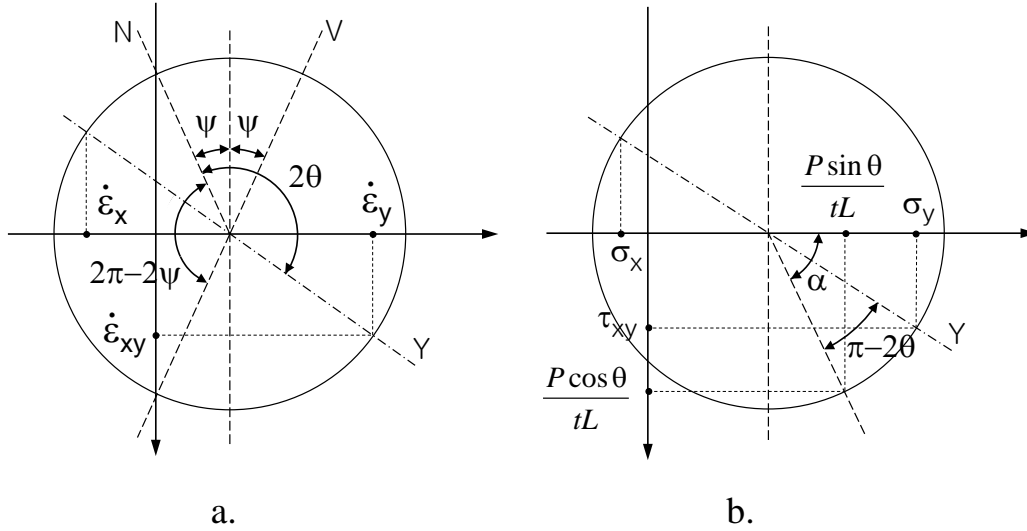


Figure 7 Mohr's circles of plastic strain rates and stresses in the neck

Based on the associativity of the flow rule, the following relationships can be derived:

$$\dot{\varepsilon}_x = \lambda \frac{\partial f}{\partial \sigma_x} = \lambda [2H(\sigma_x - \sigma_y) + 2G\sigma_x] \quad (14)$$

$$\dot{\varepsilon}_y = \lambda \frac{\partial f}{\partial \sigma_y} = \lambda [2F\sigma_y - 2H(\sigma_x - \sigma_y)] \quad (15)$$

$$\dot{\varepsilon}_{xy} = \lambda \frac{\partial f}{\partial \tau_{xy}} = \lambda [2N\tau_{xy}] \quad (16)$$

where ($f = 0$) represents the yield surface given by Eq. (9) and λ is a proportionality factor.

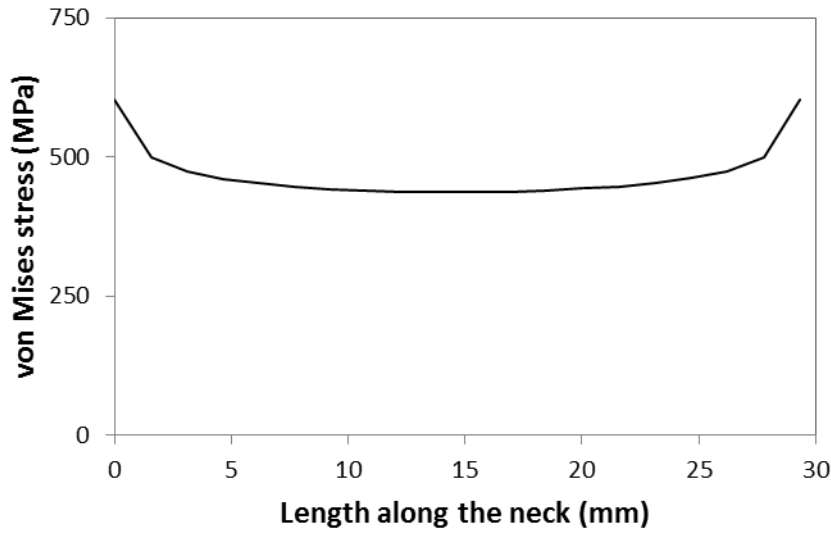


Figure 8 Stress distribution along the neck

In analogy with Hill (1953), we now assume that the stress state is uniform within the neck. This assumption has been experimentally verified by Lianis and Ford (1957) and found to be valid. It was also confirmed by the results of our preliminary FE analysis (Figure 5a and Figure 8), which showed that, with the exception of the stress concentrations at the roots of the notches, the neck is indeed in a state of nearly uniform stress. In a longitudinal cross-section of the neck the stress normal to the direction of the neck, as well as the shear stress along the direction of the neck, can then be determined from equilibrium:

$$\sigma'_y = \frac{P \sin \theta}{tL} \quad (17)$$

$$\tau'_{xy} = \frac{P \cos \theta}{tL} \quad (18)$$

These stresses determine a point on Mohr's circle of the stresses (Figure 7b). We now wish to rotate our frame of reference to determine the stresses in the x-y coordinate system, which is the only reference frame in which Eqs. (14-16) are valid. The problem is complicated, however, by the fact that in an anisotropic material the principal directions of stress and (plastic) strain rate, in general, do not coincide. Therefore the angle α (Figure 7b), which amounts to $(\pi/2-\psi)$ for an isotropic material, is initially unknown. Leaving α as an unknown for now, the stresses in the x-y reference frame are:

$$\sigma_x = \frac{P \sin \theta}{tL} - \frac{P \cos \theta}{tL \sin \alpha} [\cos \alpha - \cos(2\theta + \alpha)] \quad (19)$$

$$\sigma_y = \frac{P \sin \theta}{tL} + \frac{P \cos \theta}{tL \sin \alpha} [\cos \alpha + \cos(2\theta + \alpha)] \quad (20)$$

$$\tau_{xy} = \frac{P \cos \theta}{tL \sin \alpha} \sin(2\theta + \alpha) \quad (21)$$

The unknowns P (the load at necking) and b (the width of the neck) can be eliminated from the problem by deriving any two ratios from Eqs. (14-16) and substituting Eqs. (19-21), for example:

$$\frac{\dot{\epsilon}_y + \dot{\epsilon}_x}{\dot{\epsilon}_y - \dot{\epsilon}_x} = \frac{\sin \psi}{\sin(2\theta - \psi)} = \frac{(F + G)\cos(\alpha + \theta) + (F - G)\cos \theta \cos(2\theta + \alpha)}{(F - G)\cos(\alpha + \theta) + (F + G + 4H)\cos \theta \cos(2\theta + \alpha)} \quad (22)$$

$$\frac{\dot{\varepsilon}_y + \dot{\varepsilon}_x}{\dot{\varepsilon}_{xy}} = \frac{2 \sin \psi}{\cos(2\theta - \psi)} = -\frac{(F + G)\cos(\theta + \alpha) + (F - G)\cos \theta \cos(2\theta + \alpha)}{N \cos \theta \sin(2\theta + \alpha)} \quad (23)$$

Eliminating α from Eqs. (22-23) results in:

$$\frac{F \cos^2 \theta + G \sin^2 \theta + NB \sin \theta \cos \theta}{F(1 + 2 \cos^2 \theta) - G \cos(2\theta) - NB \cos(2\theta) / \tan \theta} = \frac{F(A - 1)\cos^2 \theta - G(A + 1)\sin^2 \theta + 2HA \cos(2\theta)}{F(A - 1)(1 + 2 \cos^2 \theta) + G(A + 1)\cos(2\theta) + 8HA \cos^2 \theta} \quad (24)$$

with:

$$A = \frac{\sin \psi}{\sin(2\theta - \psi)} \quad (25)$$

$$B = \frac{2 \sin \psi}{\cos(2\theta - \psi)} \quad (26)$$

Eq. (24) provides one relationship between the parameters F, G, H and N per test result (θ , ψ).

3 Application

When carrying out a simple tensile coupon test on an anisotropic material in a direction which includes an angle α_0 with the rolling direction, the stresses in the x-y reference frame are given by:

$$\sigma_y = s \cos^2 \alpha_0 \quad \sigma_x = s \sin^2 \alpha_0 \quad \tau_{xy} = s \sin \alpha_0 \cos \alpha_0 \quad (27)$$

where s is the applied tensile stress.

Substituting Eqs. (24) into Hill's Eq. (9) yields a relationship between F, G, H and N:

$$F \cos^4 \alpha_0 + G \sin^4 \alpha_0 + H \cos^2 2\alpha_0 + \frac{1}{2} N \sin^2 2\alpha_0 = \frac{\sigma_0^2}{s^2}$$

One could therefore wrongfully assume that the four parameters F, G, H and N can be determined by carrying out tensile tests in four independent directions including angles α_0 , β_0 , γ_0 and δ_0 with the rolling direction. However, this requires solving a system of four equations with determinant:

$$\begin{vmatrix} \cos^4 \alpha_0 & \sin^4 \alpha_0 & \cos^2 2\alpha_0 & (1/2)\sin^2 2\alpha_0 \\ \cos^4 \beta_0 & \sin^4 \beta_0 & \cos^2 2\beta_0 & (1/2)\sin^2 2\beta_0 \\ \cos^4 \gamma_0 & \sin^4 \gamma_0 & \cos^2 2\gamma_0 & (1/2)\sin^2 2\gamma_0 \\ \cos^4 \delta_0 & \sin^4 \delta_0 & \cos^2 2\delta_0 & (1/2)\sin^2 2\delta_0 \end{vmatrix} \quad (28)$$

It is easy to prove that the determinant is always zero since, for each row, the sum of the coefficients in the first and second column equals the sum of the coefficients in the third and fourth column. As a result, tensile tests in *three* different directions provide us with the maximum amount of information and a test involving applied shear is necessary to determine all four parameters. A notched strip test can be used to provide this fourth, independent relationship. This is the methodology followed in the next section to determine the yield surfaces of 304L and 430 stainless steel.

It is thereby noted that this approach provides a particular benefit for materials which are sensitive to the rate of applied loading. In the notched strip test, rather than measuring a yield load, the flow rule (i.e. the ratios between plastic strain increments) is measured. It avoids the problem of having to determine what the equivalent loading rate should be for two fundamentally different types of tests: one where the material is loaded in pure tension and one where the material is subject to combined tension and shear. As long as the relative shape of the yield surface is maintained for different rates of loading (a reasonable assumption for loading rates which are not vastly different), the notched strip tests provide compatible data with the tensile coupon tests. Notched strip tests for different angles θ (and thus different ratios of tension to shear) also provide compatible information.

4 Test Program

An experimental program was set up to investigate the feasibility of using notched strip tests to obtain information about the yield characteristics of type 304L (austenitic) and type 430 (ferritic) stainless steel sheets. The nominal thickness of the sheets was 2 mm. A total of 18 notched strip specimens including various geometries were tested. In addition, 15 conventional tensile coupons were tested. All specimens were laser-cut from AutoCAD drawings using an automated process.

In a first step, the specimens were coated with white paint to cover the highly reflective surface of the stainless steel. The choice of the paint is non-trivial as it needs to be able to accommodate significant localized straining at the neck without peeling off. Good results were obtained with a matt enamel spray paint (Plasti-Kote Projekt 102SF). Next, markers were drawn in specific locations on the specimens with a regular black pen. Circular dots, about 2 mm in diameter, were found to give the best results.

A 14 MegaPixel Canon EOS 1100D camera with a Canon 18-55mm lens was set up on a stable tripod. The camera was focussed on each test specimen before the test. While plenty of daylight was available, an extra halogen light source was installed.

The images taken by the camera were synchronized with the load output of the ESH 1000kN hydraulic test machine by a computer running LabView. A simple LabView script was written which sent a signal to the camera every 10 seconds to take a picture. Simultaneously with sending the signal, the load output was gathered from the data acquisition system and one line was written in the data file. This synchronisation is necessary to obtain useful information from the tensile coupon tests, but is unnecessary in the case of notched strip specimens, where the images alone suffice.

The images were processed using DIC software which was developed by Eberl et al. (2010) at Johns Hopkins University and Karlsruhe Institute of Technology and of which the Matlab source code has been made freely available online. The software provides the possibility of tracking several markers, defined by the user in the first image, and calculates the positions of these markers in consecutive images with sub-pixel accuracy. Based on the relative displacements of two chosen markers, strains can be calculated.

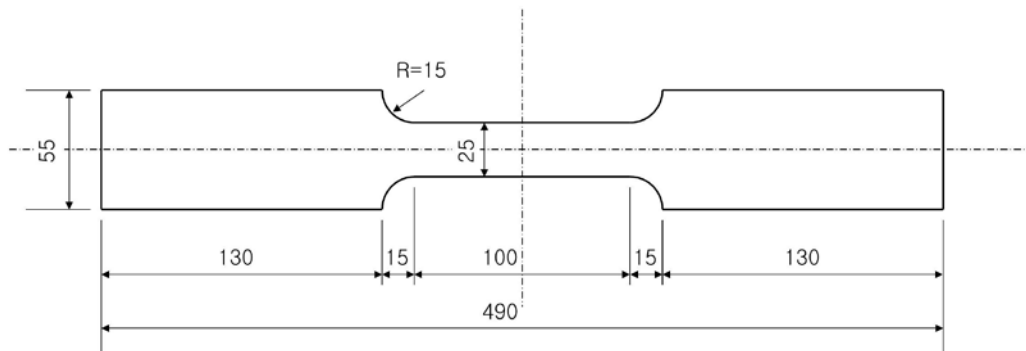


Figure 9 Nominal tensile coupon dimensions

Table 1 Ferritic tensile coupon results

Angle	Specimen	w	t	A	f_y	f_u	ϵ_u	f_y (avg)	f_u (avg)	ϵ_u (avg)
		(mm)	(mm)	(mm ²)	(MPa)	(MPa)	-	(MPa)	(MPa)	-
0°	TF-0-1	24.98	1.98	49.46	314	457	0.42	315	455	0.42
	TF-0-2	25.00	1.98	49.50	316	453	0.41			
45°	TF-45-1	25.02	1.98	49.54	345	481	0.36	340	476	0.31
	TF-45-2	25.02	1.98	49.54	334	470	0.26			
90°	TF-90-1	24.98	1.98	49.46	347	462	0.38	345	469	0.35
	TF-90-2	25.03	1.98	49.56	342	476	0.31			

Table 2 Austenitic tensile coupon results

Angle	Specimen	w	t	A	f _y	f _u	ε _u	f _y (avg)	f _u (avg)	ε _u (avg)
		(mm)	(mm)	(mm ²)	(MPa)	(MPa)	-	(MPa)	(MPa)	-
0°	TA-0-1	24.89	1.98	49.28	294	706	0.71	290	686	0.70
	TA-0-2	25.10	1.98	49.70	290	693	0.70			
	TA-0-3	24.96	1.98	49.42	287	659	0.70			
45°	TA-45-1	25.04	1.98	49.58	305	701	0.68	292	675	0.71
	TA-45-2	25.00	1.98	49.50	295	679	-			
	TA-45-3	25.00	1.98	49.50	277	645	0.73			
90°	TA-90-1	25.09	1.98	49.68	304	712	0.77	290	693	0.77
	TA-90-2	25.02	1.98	49.54	283	706	0.81			
	TA-90-3	24.96	1.98	49.28	282	661	0.72			

4.1 Tensile coupon tests

It was decided to first test the DIC technique on simple tensile coupons. Nine tensile coupons were tested for the austenitic alloy, while six coupons were tested for the ferritic alloy. Specimens were cut under three different angles with the rolling direction: 0°, 45° and 90°.

Tensile coupons were labelled with a name starting with ‘T’ (tensile coupon), followed by ‘A’ or ‘F’ (for the austenitic 304L grade or ferritic 430 grade, respectively), the angle with the rolling direction and a serial number.

Figure 9 illustrates the nominal coupon dimensions. The actual width and thickness of the coupons were measured with a micrometer screw at a number of locations along the specimen. Averaged values are presented in Tables 1 and 2.

Figure 10 shows the pattern of markers used in the DIC process. Longitudinal strains were calculated based on the two inner points along the longitudinal axis, which were a distance of approximately 50 mm apart. It was also investigated whether transverse strains could be obtained by placing two markers at half-height of the specimen at a horizontal distance of approximately 20 mm.

A displacement rate of 0.015 mm/s was initially applied in each test, which was increased to 0.1 mm/s when well past first yielding.

Figures 11 and 12 show the longitudinal and transverse stress-strain curves obtained from the tests, for the 430 alloy and 304L alloy, respectively. In general, the DIC procedure was found to be successful. As a relatively minor issue, the two austenitic coupons cut perpendicular to the rolling direction showed a 0.05 jump in strain values around a longitudinal strain of 0.3. It is unclear whether this was due to a small disturbance of the set-up, or whether the software was unable to accurately track the markers on this occasion, but it is suspected that the former was at fault. For an unknown reason, the software was also unable to track the displacements of specimen TA-45-3 past a longitudinal strain of 0.16.

Tables 1 and 2 show the 0.2% proof stress f_y , the ultimate tensile strength f_u and the ultimate strain ϵ_u (based on a 50 mm gauge length), for each ferritic and austenitic specimen, respectively. As expected, both alloys displayed good ductility, the austenitic 304L grade exhibiting ϵ_u values in excess of 70%, while the ferritic 340 grade reached at least 30% strain. The austenitic grade displayed significantly more strain hardening than the ferritic grade, a fact which also confirmed expectations. Moderate anisotropy was encountered in the ferritic sheet, with the proof stress f_y in the transverse direction exceeding the proof stress f_y in the rolling direction by 9.2% on average, while f_y in the 45° direction was on average 7.7% higher than in the rolling direction. Somewhat surprisingly, no anisotropy could be detected in the austenitic sheets when subjected to tension.



Figure 10 Typical tensile coupon (TA-45-2)

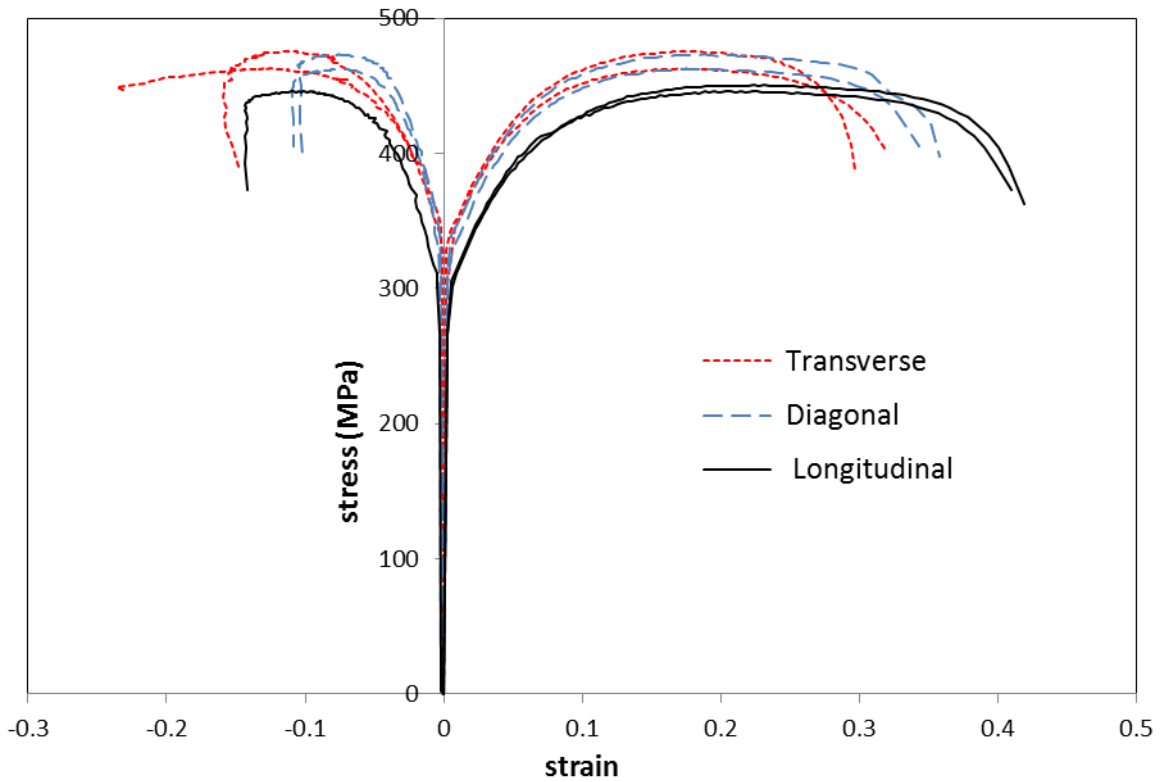


Figure 11 Ferritic grade 430 stress-strain curves

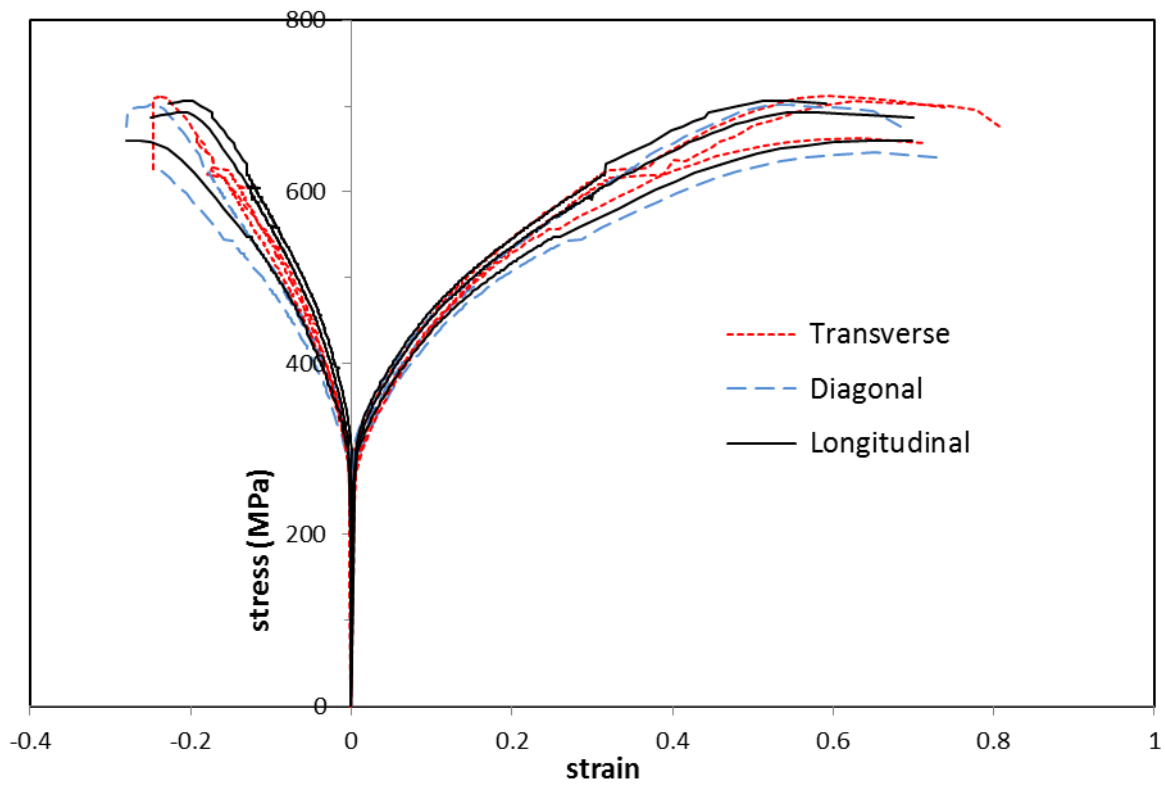
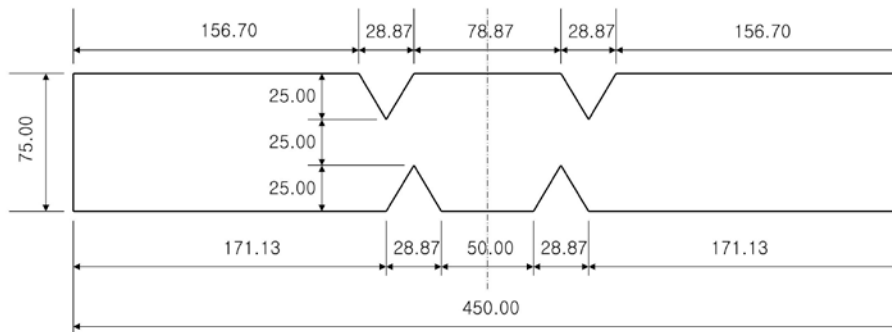
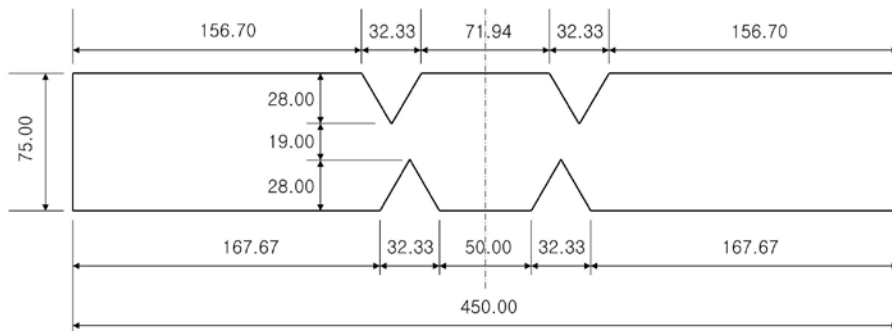


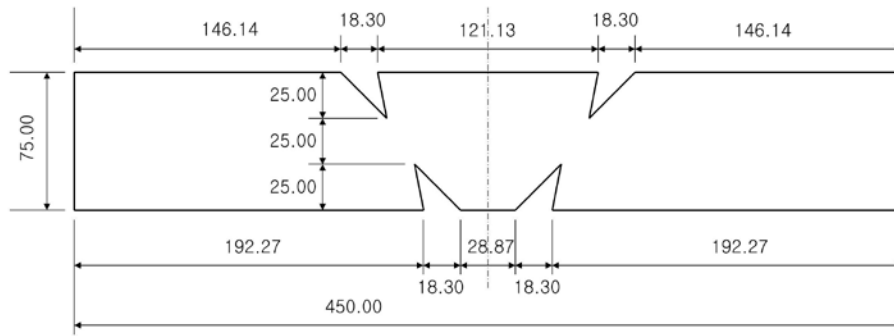
Figure 12 Austenitic grade 304L stress-strain curves



a



b



c

Figure 13 Notched strip specimen geometry

4.2 Notched strip specimens

Notched strips of three different geometries were tested (Figure 13). A first type (which we will refer to as the ‘basic’ type) incorporated the geometry previously used successfully by Hundy and Green (1954) and Lianis and Ford (1957). Figure 13a shows a basic type specimen with an angle $\theta = 60^\circ$. In this configuration, the depth of the notches is one third of the specimen width and the opening angle at the root of the notches is 60° . Because of symmetry two necks develop simultaneously in the specimen, which has the advantages that 1. It eliminates the need for hinges at the specimen ends; instead the specimen ends can be clamped into the jaws of the test machine, 2. Effectively two tests are carried out per specimen, and 3. By averaging the results obtained for the two necks, any small error due to misalignment of the specimen axis with the direction of the load can be eliminated. For both the ferritic and the austenitic alloy, three specimens of the basic type were cut along the rolling direction and three specimens were cut transverse to the rolling direction. For each direction, three values of the angle θ were considered: 60° , 70° and 80° . No angles larger than 80° were considered, because it was demonstrated by Hill (1953) that the effect of measurements errors on the strain rate ratios increases significantly past this value.

In addition, in an attempt to further promote the formation of a localized neck, two modified configurations were investigated:

- one where the depth of the notches was increased by 12% to 28mm (Figure 13b).
- one where the opening angle of the notches at the root was reduced to 30° (Figure 13c). The line connecting the roots of the notches thereby bisects this angle.

These additional coupons were only cut from the ferritic sheet in the rolling direction, but angles of 60° , 70° and 80° were considered for each type.

The specimens were identified by a name, starting with ‘N’ (indicating a notched strip specimen), followed by ‘A’ or ‘F’ (for the austenitic or ferritic grade, respectively), the angle between the longitudinal axis of the specimen and the rolling direction (in degrees), the angle θ (in degrees) and, finally, ‘B’, ‘D’ or ‘S’ (for the basic type, the type with deep notches and the type with sharp notches, respectively).

Specimen dimensions were measured with a digital vernier caliper and the average angle θ over the two necks was calculated from trigonometry.

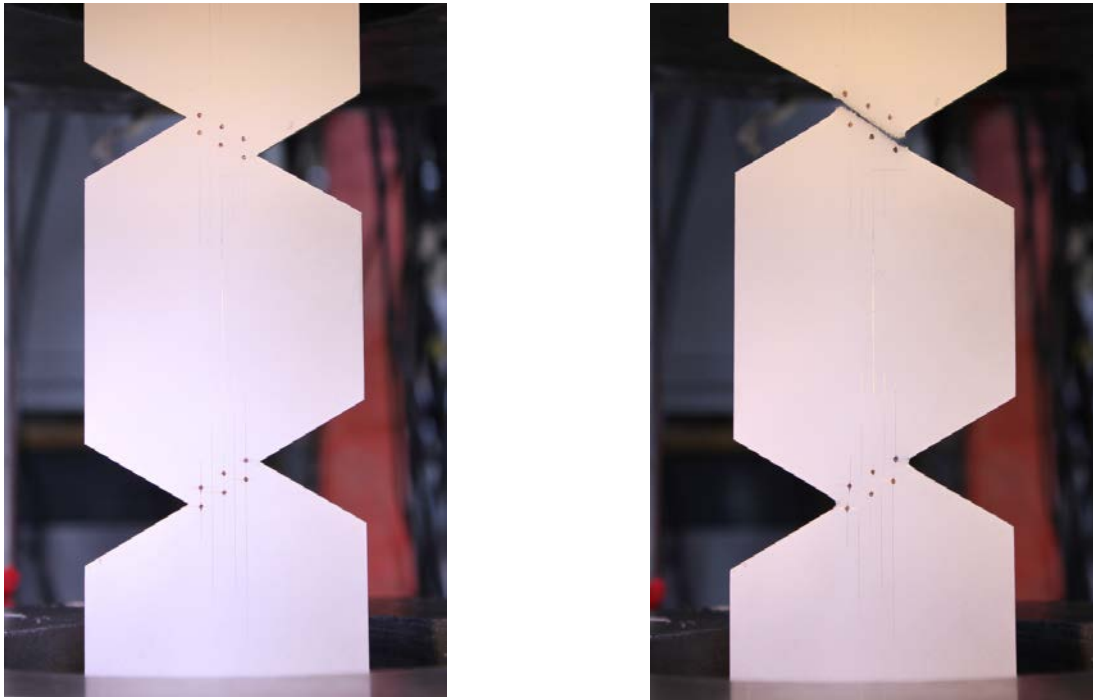


Figure 14a Typical ferritic notched strip specimen (NF-0-70-D); **b.** fracture of the neck

A consistent displacement rate of 0.003 mm/s was applied. Necking was observed in all specimens. Visually, the onset of necking could most clearly be observed on the backside of the specimen, which was not painted. The yielding was particularly localised in the ferritic specimens with the straight edges of the notches remaining fairly straight in the neighbourhood of the roots. Failure in the ferritic strips eventually took place by fracture along the neck (Figure 14a,b). In the austenitic specimens a minor amount of diffuse necking occurred, as indicated by the roots of the notches becoming more rounded. This is, of course, attributed to the higher amount of strain hardening in this material. However, a localized neck did form at higher loads. Fracture in the austenitic specimens originated from the roots of the notches with cracks propagating at right angles to the specimen axis. In some cases the cracks on either side connected to form an S-shaped failure surface (Figure 15). All specimens, ferritic and austenitic, displayed a localized neck over a sufficient range of longitudinal displacements to allow determination of the angle of relative velocity ψ .

Figure 14 shows the pattern of markers used in the DIC procedure. Dots were placed on either side of the anticipated neck at a close distance of approximately 3-4 mm from the centreline of the neck. One pair of markers was placed along the longitudinal axis of the specimen, with two more pairs being placed nearer to the notch tips. It was observed in the results that the angles ψ calculated on the basis of markers too close to the notch tips deviated by up to a few degrees from the angle ψ obtained from the markers on the longitudinal centreline. This is not entirely surprising seen the occurrence of stress concentrations near the notch tips and it is therefore recommended to use markers near the centreline. The DIC software (Eberl et al. 2010) was used to obtain relative displacements of the markers in the x- and y-directions between consecutive images, from which the angle ψ could easily be calculated.

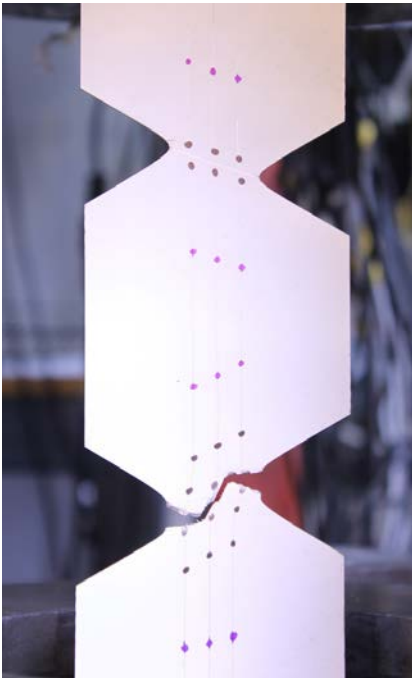
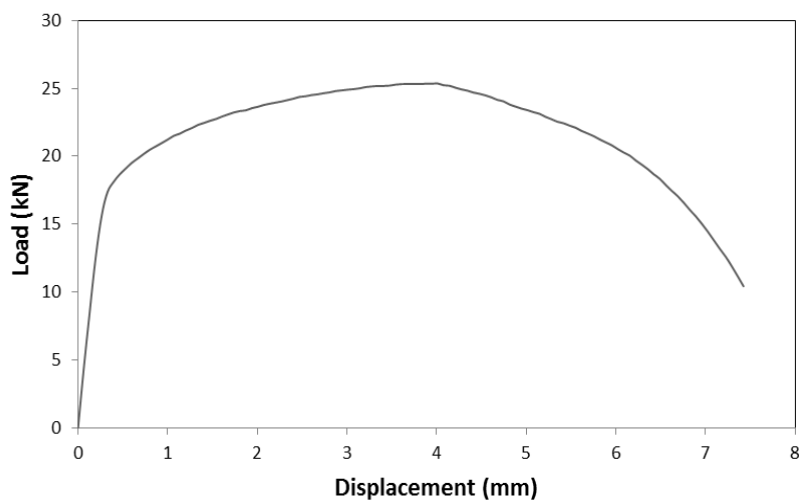


Figure 15 Fracture of an austenitic specimen (NA-90-70-B)

Figure 16 shows typical results. The angle ψ , as well as the load, are plotted against the displacements of the machine crossheads. After formation of the neck, the ψ -values show a consistent plateau which typically has a slight downwards slope. This has been confirmed by Hundy and Green (1954) who reported that the measured angle ψ only varied by about 0.5° between formation of the neck and fracture. The initial value of ψ after formation of the neck is reported in Tables 3 and 4, pertaining to the ferritic and the austenitic alloys, respectively. This initial value was considered to be the most representative of the initial yield surface, while the early stages of necking are also match the theoretical assumptions the best (in particular the assumption of plane stress). It is noted that this methodology implicitly neglects the elastic strains. Seen the slope of the load-displacement curve, the elastic strains between the closely spaced markers are very small compared to the plastic straining of the specimen, which is entirely localized in the neck. However, when choosing markers at significant distances from the neck (Figure 15), the elastic strains do cause non-negligible errors.



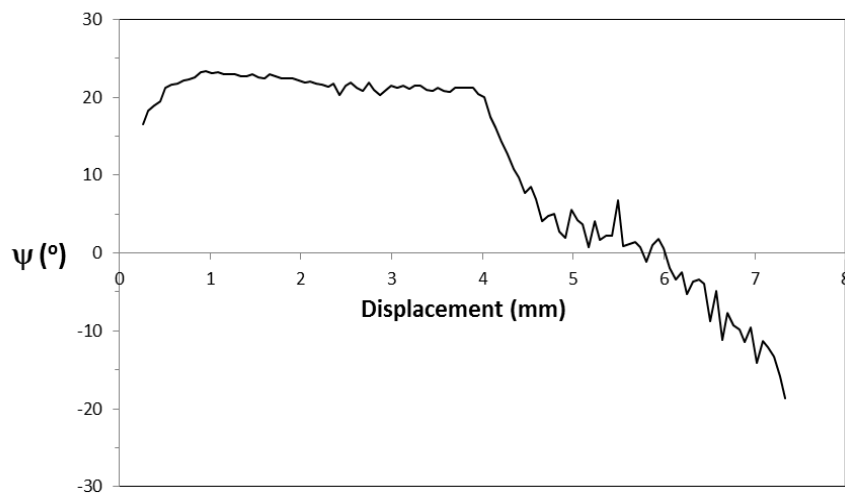


Figure 16 Typical test results

Table 3 Ferritic notched strip specimen result

Specimen	θ	ψ	ψ (theory)	F	G	H	N
	°	°	°	-	-	-	-
NF-0-60-B	60.17	26.43	23.56	0.573	0.411	0.427	1.232
NF-0-70-B	69.90	37.97	34.34	0.582	0.420	0.418	1.224
NF-0-80-B	80.30	57.50	55.63	0.555	0.393	0.445	1.251
NF-90-60-B	60.62	21.06	23.95	0.504	0.342	0.496	1.302
NF-90-70-B	70.04	31.74	34.55	0.497	0.335	0.503	1.308
NF-90-80-B	79.81	58.23	54.28	0.602	0.440	0.398	1.204
NF-0-60-D	60.36	22.72	23.72	0.480	0.318	0.520	1.326
NF-0-70-D	69.85	36.91	34.27	0.563	0.401	0.437	1.243
NF-0-80-D	80.41	54.72	55.94	0.501	0.339	0.499	1.304
NF-0-60-S	59.70	25.96	23.17	0.572	0.410	0.428	1.234
NF-0-70-S	69.92	39.75	34.37	0.616	0.454	0.384	1.189
NF-0-80-S	79.66	60.44	53.87	0.653	0.491	0.347	1.153
			Average ¹	0.540	0.378	0.460	1.266
			COV ¹	0.082	0.117	0.096	0.035

¹ Excluding the NF-0-XX-S specimens

Table 4 Austenitic notched strip specimen results

Specimen	θ	ψ	ψ (theory)	F	G	H	N
	°	°	°	-	-	-	-
NA-0-60-B	60.31	22.21	23.68	0.464	0.464	0.536	1.508
NA-0-70-B	69.86	36.22	34.29	0.534	0.534	0.466	1.438
NA-0-80-B	79.99	56.68	54.77	0.533	0.533	0.467	1.440
NA-90-60-B	59.55	26.84	23.04	0.594	0.594	0.406	1.378
NA-90-70-B	69.63	33.58	33.95	0.490	0.490	0.510	1.483
NA-90-80-B	80.12	55.84	55.13	0.509	0.509	0.491	1.464
Average				0.521	0.521	0.479	1.452
COV				0.086	0.086	0.093	0.031

Tables 3 and 4 list the measured angle θ and the measured angle ψ for each specimen, as well as the theoretical value of ψ , assuming an isotropic material. For the ferritic specimens, the measured angle ψ is on average larger than the isotropic angle ψ for specimens where the longitudinal axis corresponds with the rolling direction, while the measured angle ψ is on average lower than the isotropic angle ψ when the longitudinal specimen axis is oriented transverse to the rolling direction. This is to be expected for an anisotropic material where the transverse direction exhibits the higher yield stress. For the austenitic specimens, the resulting angles ψ are closer, on average, to the angles predicted for an isotropic material. This observation is consistent with the tensile coupon results.

The 'D'-type ferritic specimens with deeper notches yielded slightly lower ψ -values on average. Seen the limited amount of specimens tested, however, the results could statistically not be considered to be significantly different from the results of the basic specimens, suggesting for now that either type may be used. However, the 'S'-type specimens with sharp 30° notches yielded results which differed more substantially from the results of the 'B' and 'D'-type specimens, with the inconsistency increasing for increasing values of θ . It is suspected that this is due to the introduction of a more significant end effect at the roots of the notches and it is therefore recommended that this geometry not be used.

5 Analysis

The method previously explained in Section 3 was used to determine the coefficients F, G, H and N of Hill's yield surface (Eq. 9) for the ferritic 430 alloy as well as for the austenitic 304L alloy. Three relationships between the coefficients were obtained from the tensile coupon results. For instance, for the ferritic alloy (with the reference stress σ_0 in Eq. 9 chosen equal to the yield stress in the rolling direction), substitution into Eq. (9) of the test data in the rolling, transverse and diagonal directions yielded the respective equations:

$$F + H = 1 \quad (29)$$

$$G + H = (315/345)^2 = 0.838 \quad (30)$$

$$F + G + 2N = 4(315/340)^2 = 3.449 \quad (31)$$

A fourth equation was provided by Eq. (24), with A and B calculated for a particular data set (θ, ψ). After elimination of F, G and H, Eq. (24) becomes a quadratic equation in N. This procedure was carried out for all test points and the resulting coefficients are listed in Tables 3 (for the ferritic alloy) and 4 (for the austenitic alloy). Averages were calculated (excluding the 'S'-type specimens) and yielded the following coefficients for the ferritic alloy: F = 0.54; G = 0.38; H = 0.46 and N = 1.27. For the austenitic alloy the averages were much closer to the isotropic values with F = 0.52; G = 0.52; H = 0.48 and N = 1.45. A considerable spread in the results was observed, as illustrated by the coefficients of variation (COV) listed in Tables 3 and 4. The underlying variation in ψ appears to be typical for the test method, independent of the measuring method used and has been confirmed by other researchers (Baraya and Parker 1963). It may be caused by the fact that only a very localized area of the material is subjected to yielding and that, consequently, local defects and spatial variations in the material strength play a significant role. A sufficient number of tests therefore need to be carried out.

6 Check

The fact that transverse strains as well as longitudinal strains were measured in the tensile coupons, in principle, allows for a check to be carried out on the results obtained in section 5. Indeed, when subjecting the material to tension in the y-direction (rolling direction), Eqs. (14-16) demand that the ratio of the plastic strain rate in the x-direction to the plastic strain rate in the y-direction is given by:

$$\frac{\dot{\epsilon}_{x,p}}{\dot{\epsilon}_{y,p}} = -\frac{H}{F+H} \quad (32)$$

Similarly, when subjecting the material to tension in the x-direction, the corresponding ratio is given by:

$$\frac{\dot{\epsilon}_{y,p}}{\dot{\epsilon}_{x,p}} = -\frac{H}{G+H} \quad (33)$$

Using the coupon test data, it was found that this check was difficult to carry out. The ratios of the plastic strain increments were typically subject to a large amount of measuring noise associated with the need to track two different pairs of points. Moreover, the ratios needed to be calculated before any localisation of plasticity occurred in the specimen. No sufficiently reliable results could be extracted and the values listed in Table 5 should be considered approximate.

Table 5 Comparison of the plastic strain rate ratios

	Ferritic		Austenitic	
	-H/(F+H)	-H/(G+H)	-H/(F+H)	-H/(G+H)
Section 5	-0.46	-0.55	-0.48	-0.48
Eqs. (32-33)	-0.52	-0.59	-0.48	-0.56
Difference (%)	13.0	7.3	0.0	16.7

Conclusions

When proposing the concept of notched strip tensile tests to investigate the yield characteristics of metals, Hill (1953) envisioned a test which would satisfy three criteria: 1. A simple test apparatus, 2. Easily fabricated specimens, and 3. An easy test procedure. While the first two criteria were satisfied from inception, it is here demonstrated that DIC techniques can be added to the test to considerably facilitate an accurate measurement of the angle of relative velocity ψ . In addition, new theoretical developments are presented, which eliminate the need for a measurement of the yield load and which allow the yield surface of an anisotropic material to be determined starting from a parameterized equation. It suffices that images are taken of the specimen at sufficiently short (but not necessarily regular) intervals. The angle θ of the anticipated neck is the only dimensional measurement required. A disadvantage of the method lies in the relatively high scatter in ψ -values encountered.

The new techniques are illustrated by successfully employing them to determine the yield surfaces of type 430 ferritic and type 304L austenitic stainless steel.

Acknowledgement

The authors would like to extend their gratitude towards Outokumpu Sheffield, in particular Mr. Jamie Sharp, for their support of this research through the donation of the materials used in the experimental program.

References

ABAQUS User's Manual (2010), version 6.10.

<https://www.sharcnet.ca/Software/Abaqus610/Documentation/docs/v6.10/index.html>

AISI (1974). *Steel Products Manual – Stainless and Heat Resisting Steels*, American Iron and Steel Institute, Washington, D.C.

Baraya, G.L., and Parker, J. (1963). "Determination of yield surfaces by notched strip specimens." *International Journal of Mechanical Sciences*, 5, 353-363.

Becque, J., and Rasmussen, K.J.R. (2009) "Experimental Investigation of Local-Overall Interaction Buckling of Stainless Steel Lipped Channel Columns." *Journal of Constructional Steel Research*, 65 (8-9), pp. 1677-1684.

- Bijlaard, P.P. (1940). "Theory of local plastic deformations." *Publications of the International Association for Bridge and Structural Engineers* 6, 27.
- Davis, E.A. (1943). *Transactions of the American Society of Mechanical Engineers* 65, A-187.
- Eberl, C., Thompson R., Gianola, D., and Bundschuh, S. (2010). "Digital Image Correlation and Tracking with Matlab." <http://www.mathworks.com/matlabcentral/fileexchange/12413-digital-image-correlation-and-tracking>
- EN-10088-1 (2005). *Stainless Steels; Part 1: List of stainless steels*, European Committee for Standardisation, Brussels.
- Fraenkel, S.J. (1948). "Experimental studies of biaxially stressed mild steel in the plastic range." *Journal of Applied Mechanics - Transactions of the ASME* 15 (3), 193-200.
- Hill, R. (1950). *The Mathematical Theory of Plasticity*, Oxford University Press, London.
- Hill, R. (1952). "On discontinuous plastic states, with special reference to localized necking in thin sheets." *Journal of the Mechanics and Physics of Solids*, 1, 19-30.
- Hill, R. (1953). "A new method for determining the yield criterion and plastic potential of ductile metals." *Journal of the Mechanics and Physics of Solids* 1 (4), 271-276.
- Hundy, B.B., and Green, A.P. (1954). "A determination of plastic stress-strain relations." *Journal of the Mechanics and Physics of Solids*, 3, 16-21.
- Lianis, G., and Ford, H. (1957). "An experimental investigation of the yield criterion and the stress-strain law." *Journal of the Mechanics and Physics of Solids*, 5, 215-222.
- Lode, W. (1926). "Trial on the influence of the middle principle stress on the flow of metal iron, copper and nickel." *Zeitschrift fur Physik* 36 (11/12), 913-939.
- Schmidt, R. (1932). *Ingenieur-Archiv* 3, 215.
- Taylor, G.I., and Quinney, H. (1932). "The plastic distortion of metals." *Philosophical Transactions of the Royal Society of London, Series A – Containing Papers of a Mathematical or Physical Character* 230, 323-362.